SANDIA REPORT

SAND2015-XXXX Unlimited Release Printed November 2015

EMR Coupling into Systems: Calibration of the Sandia Reverberation Chamber and Validation of the Single Slot Aperture Gain Model

Mark Jursich

Prepared by Sandia National Laboratories Albuquerque, New Mexico 87185 and Livermore, California 94550

Sandia National Laboratories is a multi-program laboratory managed and operated by Sandia Corporation, a wholly owned subsidiary of Lockheed Martin Corporation, for the U.S. Department of Energy's National Nuclear Security Administration under contract DE-AC04-94AL85000.

12501016

Approved for public release; further dissemination unlimited.



Issued by Sandia National Laboratories, operated for the United States Department of Energy by Sandia Corporation.

NOTICE: This report was prepared as an account of work sponsored by an agency of the United States Government. Neither the United States Government, nor any agency thereof, nor any of their employees, nor any of their contractors, subcontractors, or their employees, make any warranty, express or implied, or assume any legal liability or responsibility for the accuracy, completeness, or usefulness of any information, apparatus, product, or process disclosed, or represent that its use would not infringe privately owned rights. Reference herein to any specific commercial product, process, or service by trade name, trademark, manufacturer, or otherwise, does not necessarily constitute or imply its endorsement, recommendation, or favoring by the United States Government, any agency thereof, or any of their contractors or subcontractors. The views and opinions expressed herein do not necessarily state or reflect those of the United States Government, any agency thereof, or any of their contractors.

Printed in the United States of America. This report has been reproduced directly from the best available copy.

Available to DOE and DOE contractors from

U.S. Department of Energy Office of Scientific and Technical Information P.O. Box 62 Oak Ridge, TN 37831

Telephone: (865) 576-8401 Facsimile: (865) 576-5728

E-Mail: reports@adonis.osti.gov Online ordering: http://www.osti.gov/bridge

Available to the public from

U.S. Department of Commerce National Technical Information Service 5285 Port Royal Rd. Springfield, VA 22161

Telephone: (800) 553-6847 Facsimile: (703) 605-6900

E-Mail: <u>orders@ntis.fedworld.gov</u>

Online order: http://www.ntis.gov/help/ordermethods.asp?loc=7-4-0#online



SAND2015-XXXX Unlimited Release Printed November 2015

EMR COUPLING INTO SYSTEMS: CALIBRATION OF THE SANDIA REVERBERATION CHAMBER AND VALIDATION OF THE SINGLE SLOT APERTURE GAIN MODEL

Mark Jursich
Electrical Science and Experiments
Sandia National Laboratories
P.O. Box 5800
Albuquerque, New Mexico 87185-MS1152

Abstract

Electromagnetic threats to weapon systems are always specified in terms of an incident plane wave. Sandia strongly prefers to test electromagnetic susceptibility in a reverberation chamber because a reverberant environment does not allow any potential point of entry to be shadowed. At the same time, a reverberation chamber averages out the directive gain of any points of entry. This would result in an under test of the system. Subsequently, a plane wave correction factor is needed to relate the plane wave and reverberation environments. Warne, et al, at Sandia have developed a theoretical correction factor and a previous attempt to validate it using an anechoic chamber (Higgins & Charley, Electromagnetic Radiation (EMR) Coupling into Complex Systems Aperture Coupling into Canonical Cavities in Reverberant and Anechoic Environments and Model Validation (SAND2007-7391), 2007) was not conclusive. In this current work the theoretical factor has been validated by creating the plane wave environment inside a gigahertz transverse electromagnetic (GTEM) cell instead of an anechoic chamber. The correlation is excellent at all but the lowest frequencies tested. The discrepancy in the low frequency regime is understood in terms of limits on the test capabilities.

ACKNOWLEDGMENTS

The author would to acknowledge the invaluable help of Mr. Joshua Usher who constructed the stirrer system used in the test object described in Section 2.2.

CONTENTS

		igle Slot Aperture Gain Model				
1.	9 8	Introduction.				
	1.1.	Description of the Sandia National Laboratories Reverberation Chamber				
	1.2. 1.3.	MIL-STD-461F Calibration				
	1.3. 1.4.	IEC 61000-4-21 Calibration				
	1.4.	Verification Using Calibrated Field Probe.				
	1.5.	-				
2.		Slot Gain Correction Validation				
		2.1 Validation of the Plane Wave Correction Factor				
	2.2 In	ternal Stirrer Test	25			
3.		Conclusion	27			
4.		References.	29			
5.		Distribution	30			
Ľ:		FIGURES	10			
		Sandia reverberation chamber showing the stirrer				
Figure 2: Q for the Sandia reverberation chamber						
Figure 3: Placement of field probes in the DO-160G test						
Figure 4: Results of DO-160G field variation test						
Figure 6: 4.3 mm (left) and 0 length (right) monopoles						
		Average predicted and measured fields. The jump in the E field at 18 GHz is due to a				
amplifier change						
		Peak measured and predicted fields. The jump in the E field at 18 GHz is due to an				
		change				
Figure 9: Canonical test object in the GTEM cell.						
Figure 10: Test object in the reverberation chamber						
Figure 11: Uncorrected shielding effectiveness measurements. Below 1.5 GHz the GTEM SE is						
		y degraded because the measurement instrumentation is at its noise floor				
		: Shielding effectiveness comparison with NIST correction factor applied. Below 1.5				
		GTEM SE is artificially degraded because the measurement instrumentation is at its				
		or				
		: Shielding effectiveness comparison with Sandia correction factor applied. Below 1.	5			
		GTEM SE is artificially degraded because the measurement instrumentation is at its	24			
		or: : Internal stirrer for the canonical test object				
-		: Internal stirrer for the canonical test object: : Internal stirrer test results. Data smoothing was applied to each case to help	43			
		sh the data trends.	26			

NOMENCLATURE

dB decibel

DOE Department of Energy EMR Electromagnetic radiation

GHz Gigahertz

GTEM Gigahertz transverse electromagnetic cell

MHz Megahertz

MSC Mode-stirred chamber, also known as a reverberation chamber

NW Nuclear weapon

SNL Sandia National Laboratories

WSEAT Weapons system engineering advanced technology

1. INTRODUCTION

Electromagnetic Radiation (EMR) leakage into nuclear weapon systems can cause upset of time-and/or mission-critical functions, damage critical electronics, or affect electro-explosive devices. The objective of the EMR Coupling into Systems project is to characterize electromagnetic leakage into the interior of systems. The ultimate goal of this project is to provide a means of predicting pin-level excitations (voltages or currents) incident on a component interface within a complex system (i.e. a weapon) when the exterior of the system is exposed to EMR. This predictive capability can be used as a tool to define/refine component level requirements, assess systems when new environments are specified, optimize new designs, assist in rapid turnaround of prototype designs and troubleshooting, and assist in component- and system-level certification.

The first purpose of this report is to document results reported previously in WSEAT news notes, as well as to present new data on the verification of wall mounted field sensors used in the operation of Sandia's reverberation chamber. The second purpose is to present validation data on the reverberation chamber gain correction factor.

1.1. Description of the Sandia National Laboratories Reverberation Chamber

The Sandia reverberation chamber is a 4x7x11 m welded aluminum chamber. RF/microwave energy is injected into the chamber via a series of antennas driven by high power amplifiers. Currently, these amplifiers cover the frequency range of 80 MHz to 40 GHz. The chamber is intended to be operated in a highly over-moded condition. As a result, the lowest useable frequency (LUF) will be greater than 80 MHz. This will be discussed in sections 1.1 through 1.4 below. The system also includes a large aluminum stirrer whose function is to homogenize the distribution of electrical energy within the chamber. Reverberation chambers are often referred to as mode-stirred chambers, but the term, *reverberation chamber*, is generally considered more descriptive. A photograph of the interior of the Sandia chamber is shown in Figure 1.



Figure 1 Sandia reverberation chamber showing the stirrer.

The high conductivity walls of the Sandia chamber result in an enhanced ability to store electrical energy. The measure of the ability to store energy is known as chamber Q. Numerically, Q is given by

$$Q = \frac{2\pi f W_s}{P_l}.$$

In the equation above, f is frequency, W_s is stored energy, and P_l is power loss. An excellent discussion of chamber Q can be found in Hill. (Hill, 2009). Q for the Sandia reverberation chamber is shown in Figure 2.

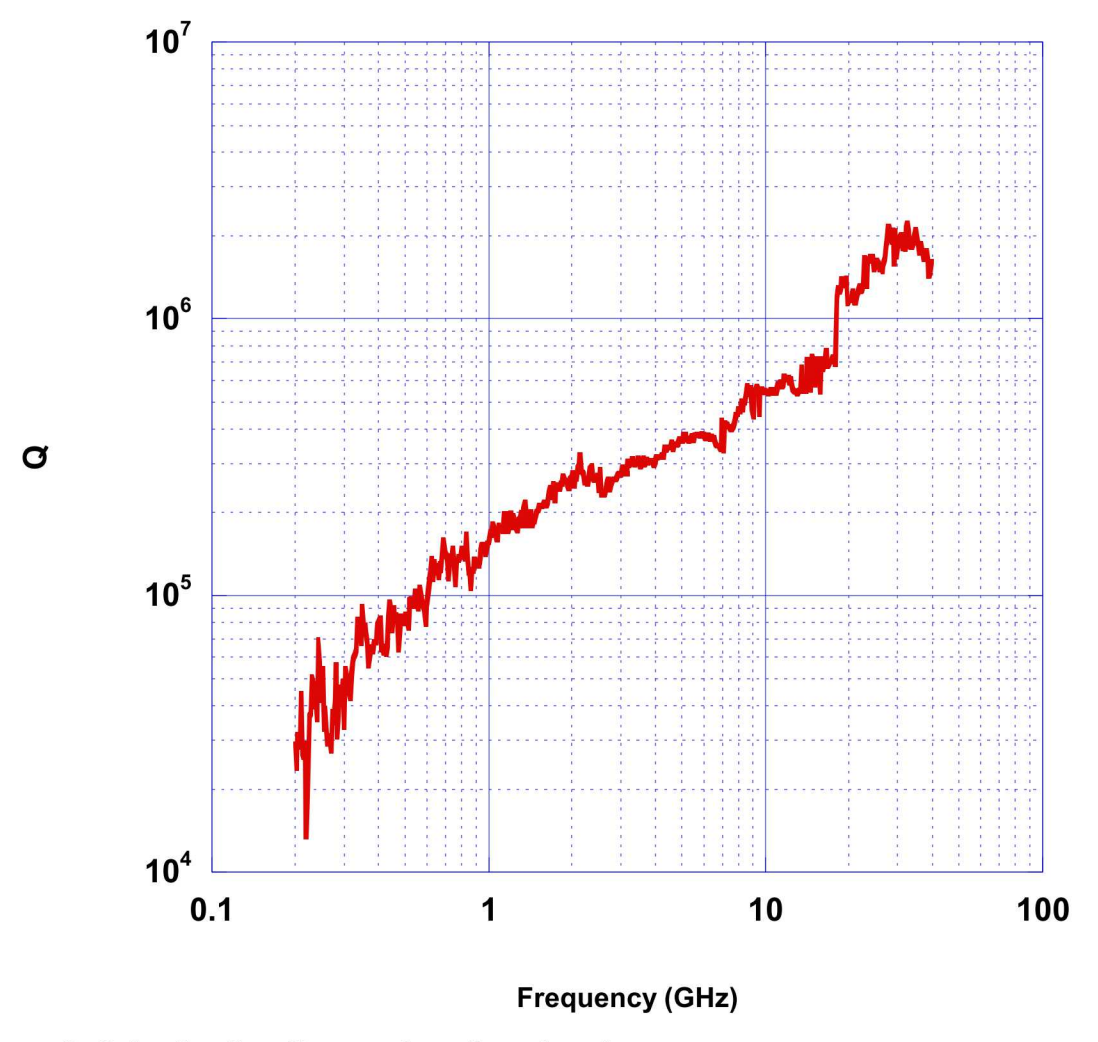


Figure 2: Q for the Sandia reverberation chamber

One important advantage to a high Q chamber is that very high electric field strengths can be achieved. This is important in Sandia's susceptibility testing. However, it also limits the lowest usable frequency at which the chamber can be operated.

1.2. MIL-STD-461F Calibration

The military standard (MIL-STD-461F, 2007) does not provide guidance on how to determine the LUF of any particular chamber based on a verification measurement. The criterion is basically that 100 simultaneous modes must exist. The theoretical number of modes is estimated by

$$N = \frac{8\pi}{3} abd \frac{f^3}{c^3}.$$

Here a, b, and d are the chamber internal dimensions in meters, f is the operation frequency in Hz, and c is the speed of propagation (3 x 10⁸ m/s). Based on this criterion, Sandia's chamber could be operated down to 100 MHz. However, this criterion does not allow for the known problem of degenerate modes. Denegerate modes result in large inhomogenieties in the fields within the chamber, which is undesirable. In order to reduce the number of degenerate modes, modern reverberation chambers are designed so that the dimensions are not integral multiples of one another. The criterion above does not reflect this.

1.3. RTCA DO-160G Calibration

The Radio Technical Commission for Aeronautics¹ (RTCA) has published a standard (DO-160G, 2010) which is based on limiting the electric field inhomogeneity within the chamber. The criterion is based on a direct measurement of the spatial variation of electric field. Following the RTCA standard, a calibrated 3-axis electric field probe was placed at each of the eight corners and at the center of the proposed working volume of the chamber. All three components of the electric field were measured using an ETS Lindgren Model 6153 10 MHz to 40 GHz isotropic probe at approximately 0.36 degree increments of the stirrer rotation. Average and peak field levels were recorded for a complete stirrer rotation at each frequency and at each position in the chamber. A receive antenna was also placed in the test volume to monitor power. A top down view of this configuration is shown in Figure 3 below. Note that the probe locations are 1.5 meters from the chamber walls. The distance from the floor and ceiling of the chamber was 1 m.

The RTCA criterion is based on the total variation of the peak field measurements over the 9 locations. The data and corresponding limit are shown in Figure 4. According to this standard, the Sandia reverberation chamber is usable down to the lowest frequency tested, i.e. 100 MHz.

¹ RTCA, Inc. is a US volunteer organization that develops technical guidance for use by government regulatory authorities and by industry.

_

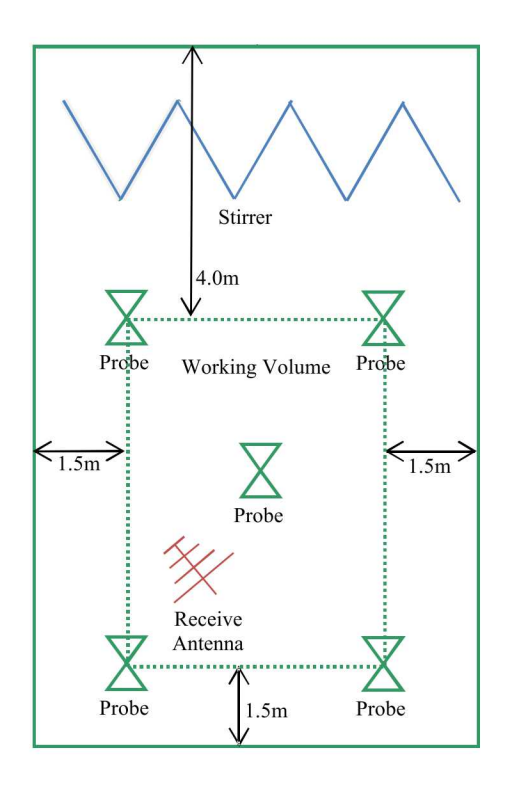


Figure 3: Placement of field probes in the DO-160G test

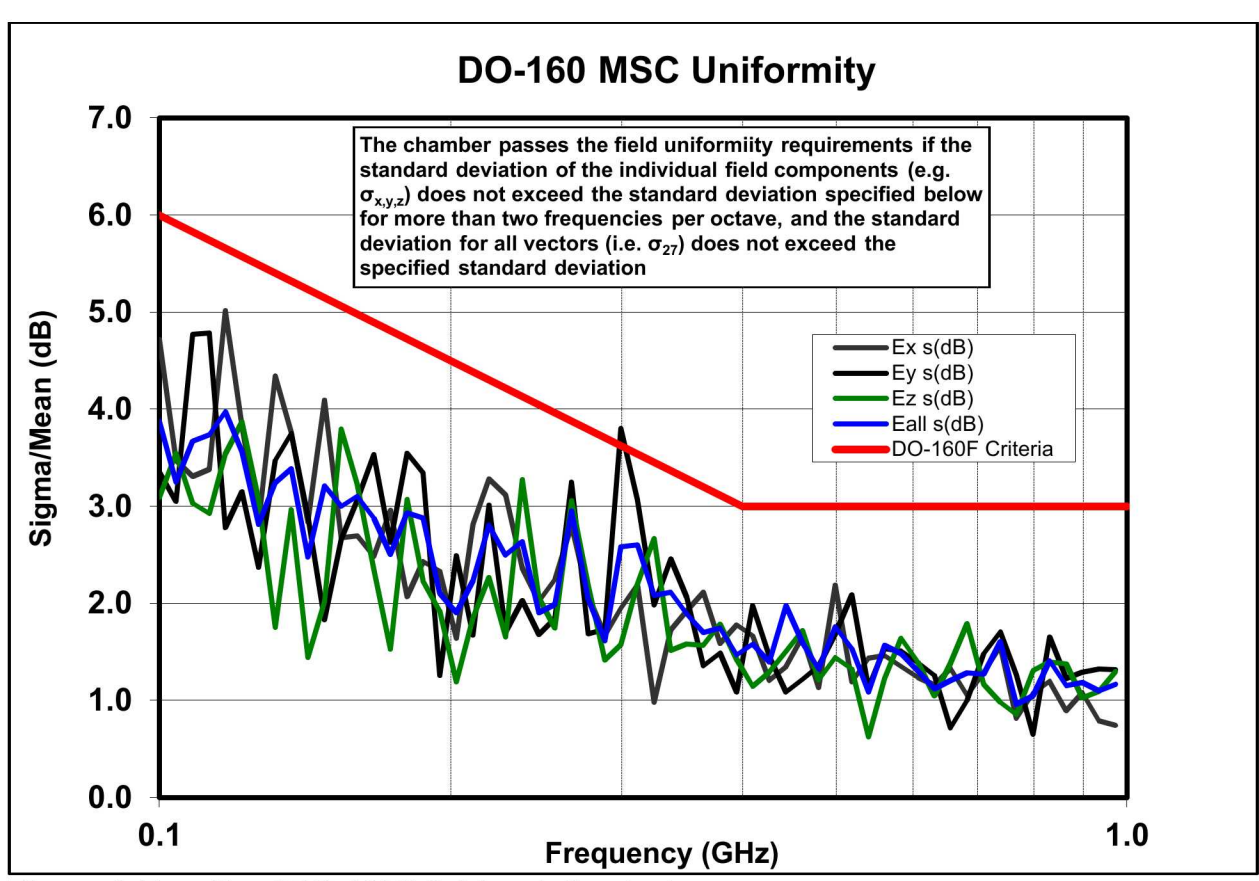


Figure 4: Results of DO-160G field variation test

1.4. IEC 61000-4-21 Calibration

The International Electrotechnical Commission (IEC) has also published similar standard (IEC 61000-4-21, 2011). This standard is almost identical to the RTCA except for two things. First the specification limit is more restrictive, allowing only 4 dB variation at 100 MHz instead of 6 dB. Secondly, the probe location at the center of the working volume is eliminated and the variance is calculated over the remaining 8 points.

The results of this test are shown in Figure 5 along with the IEC criteria. In this case the chamber would be considered usable down to ~135 MHz. During testing the Sandia chamber is always operated above 150 and usually above 200MHz.

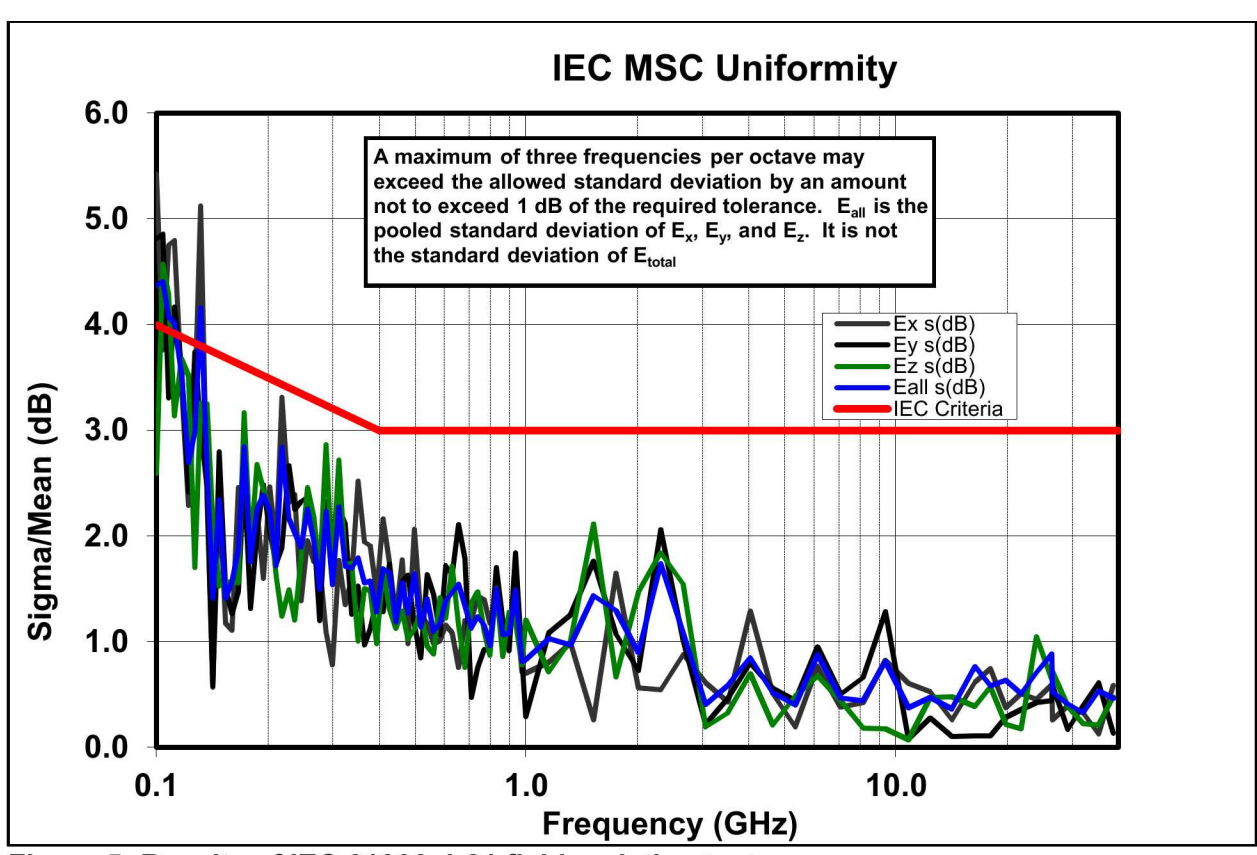


Figure 5: Results of IEC 61000-4-21 field variation test

1.5. Verification Using Calibrated Field Probe

The normal procedure for monitoring the electric field in a reverberation chamber would be to use a calibrated receive antenna within the working volume. This represents two problems in Sandia's testing First, a receive antenna will load the chamber and reduce the maximum achievable electric field. Secondly, it is common for Sandia to test rather large objects and a separate receive antenna simply gets in the way. Wall mounted monopole probes avoid both of these issues. Below 18 GHz a series of four 4.3 mm monopole probes are used to monitor the chamber field. Above 18 GHz a set of four zero length monopoles are used. These are shown in Figure 6.

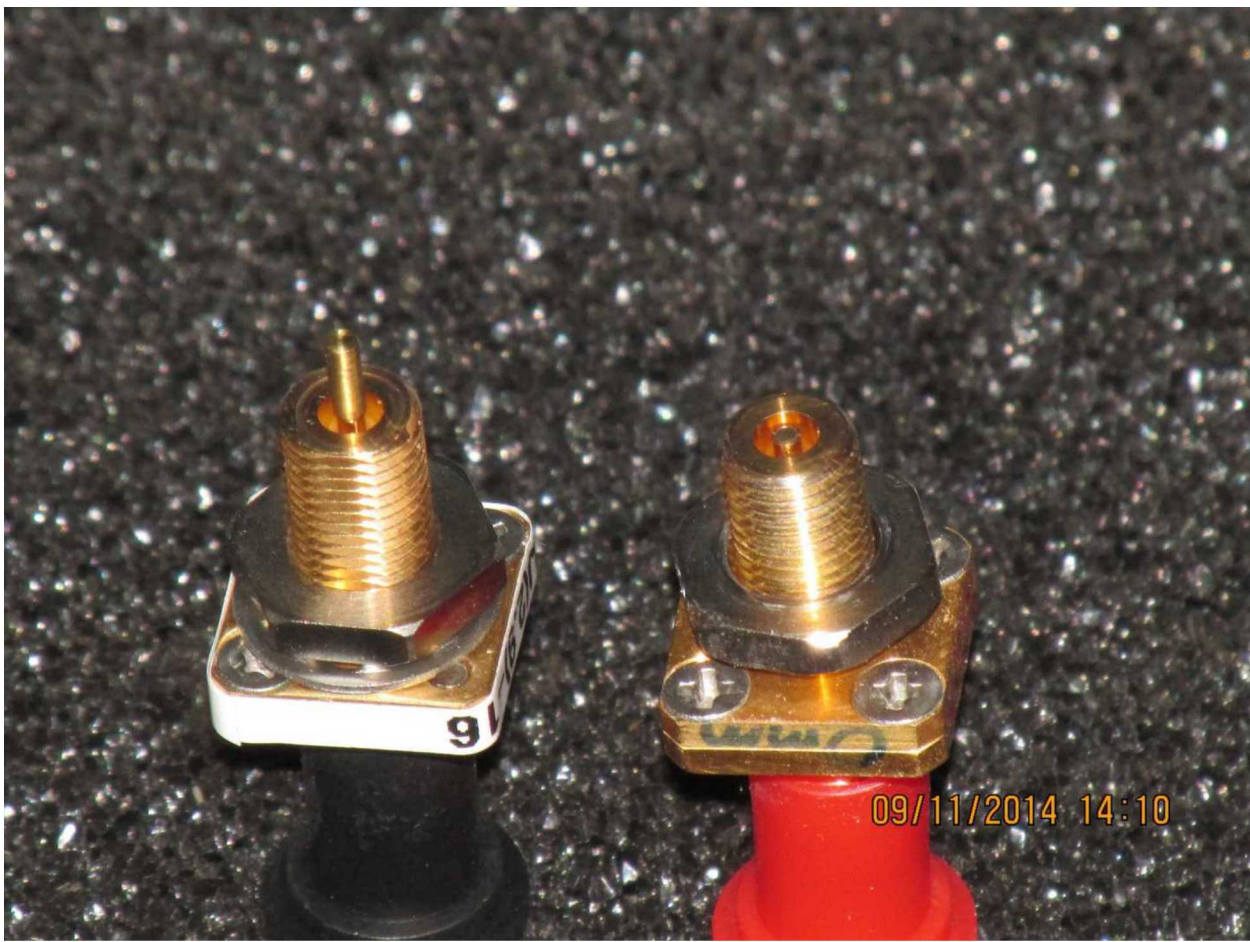


Figure 6: 4.3 mm (left) and 0 length (right) monopoles

These monopoles have been used for some time at Sandia and are understood quite well. Nevertheless, verification of the electric field predictions based on these wall sensors is in order, because the wall sensors are outside the actual working volume of the chamber. Therefore a test was run in which a calibrated field probe (ETS 6153) was placed in the center of the working volume. The measured electric field was then compared to the electric field predictions based on the wall sensors. These data are shown in Figure 7 and Figure 8. In the figures, the terms, average and peak, refer to the average and peak over one rotation of the stirrer and not a time average. In general, the correlation is quite good with the maximum deviations over all frequencies ~1.5 dB.

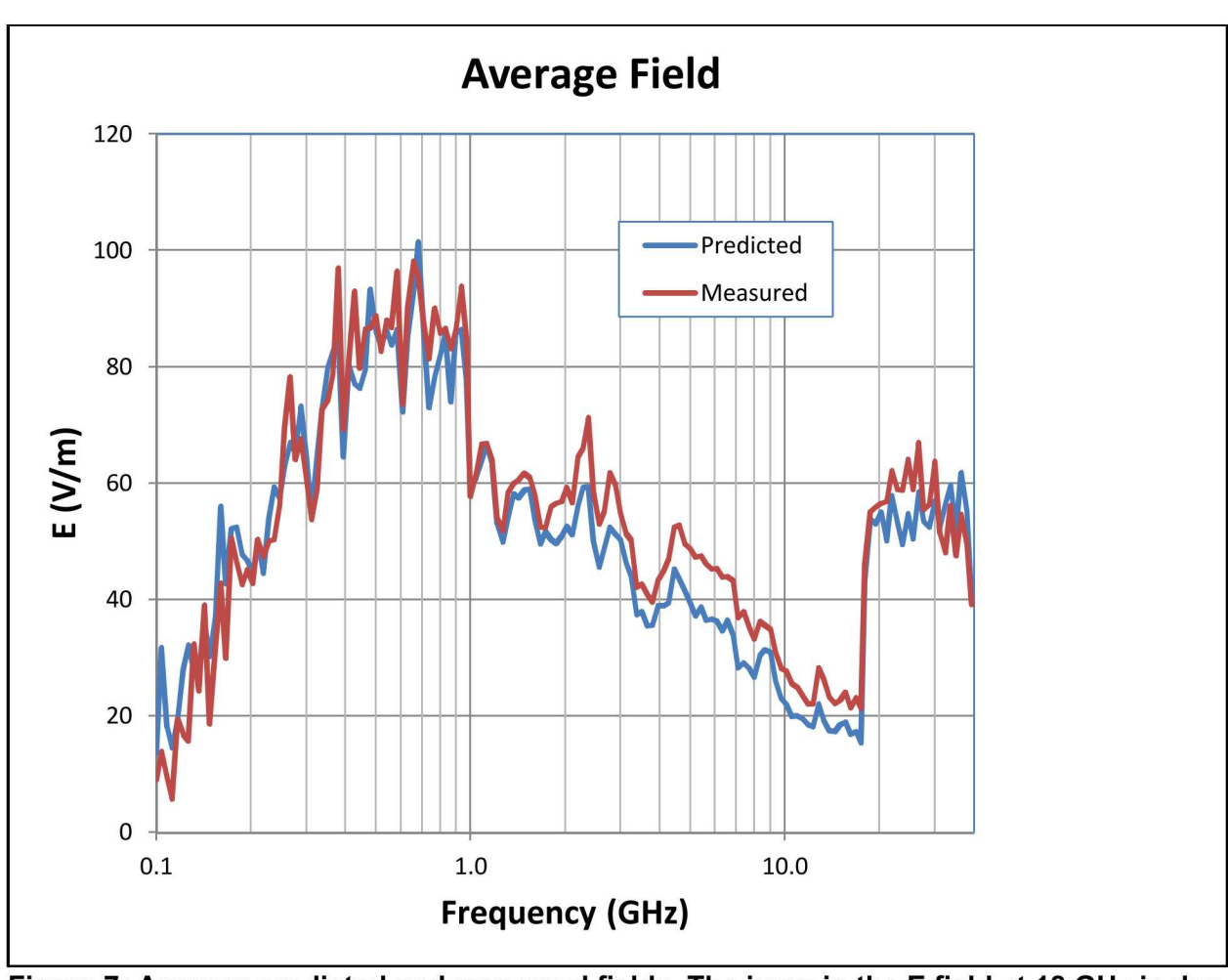


Figure 7: Average predicted and measured fields. The jump in the E field at 18 GHz is due to an amplifier change.

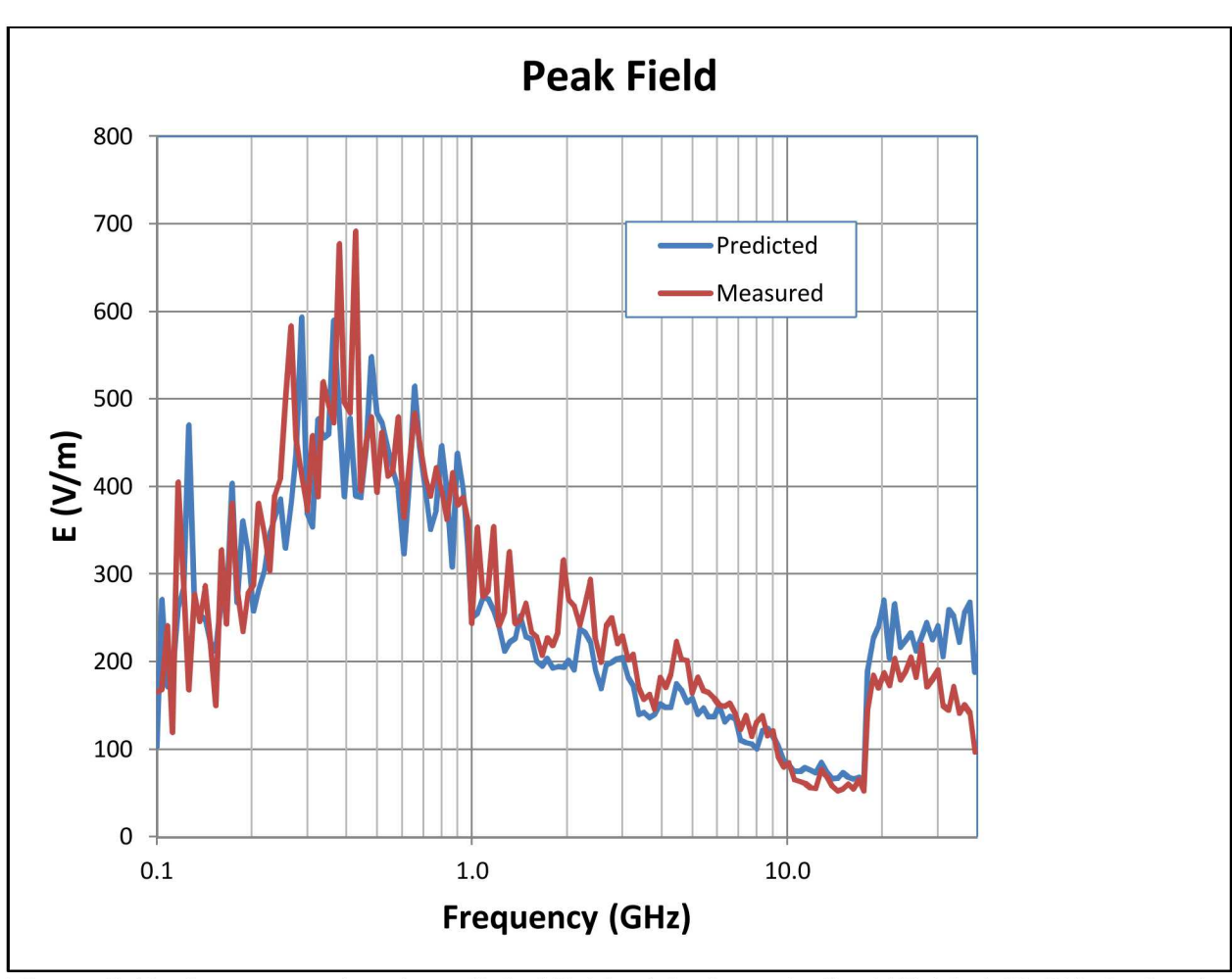


Figure 8: Peak measured and predicted fields. The jump in the E field at 18 GHz is due to an amplifier change.

2. SLOT GAIN CORRECTION VALIDATION

2.1 Validation of the Plane Wave Correction Factor

In this work the slot gain correction factors developed by Warne, et al, at Sandia and another developed at NIST (Koepke, Hill, & Ladbury, 1996) were tested using a canonical test device described earlier (Higgins & Charley, Electromagnetic Radiation (EMR) Coupling into Complex Systems Aperture Coupling into Canonical Cavities in Reverberant and Anechoic Environments and Model Validation (SAND2007-7391), 2007). The test object was a 9"x17"x25" welded aluminum box with a single slot in the center of the lid. The slot dimensions were 0.05"x2.5". A complete description of the test object can be found in the Higgins report. In this work only the single slot configuration was tested. A picture of the test object in the GTEM is shown in Figure 9.



Figure 9: Canonical test object in the GTEM cell.

In contrast with the previous work, the plane wave environment was produced in an ETS-Lindgren 0.75 meter GTEM cell. The test object was oriented with the slot at normal incidence to the incoming wave. The electric field was along the easy axis of the slot. The electric field interior to the cavity was measured using a 4.3 mm monopole. The external field was measured using a second monopole protruding from the box. The second monopole can be seen in Figure

9. The shielding effectiveness is the ratio of internal to external field. In this case it can also be calculated as the ratio of the received power of the two monopoles. An ETS 6153 field probe was also placed in the chamber to cross-check the field predictions derived from the external monopole. All the measured results were consistent.

The test object was then placed in the reverberation chamber and the shielding effectiveness measured as the ratio of the received power of the two monopoles. The test object in the mode stirred chamber is shown in Figure 1.



Figure 10: Test object in the reverberation chamber

In this case the external monopole data was cross checked against the wall mounted sensors described in section 1.5. Again, the measurements were all consistent.

The shielding effectiveness measurements with no gain correction factor applied are shown in Figure 11.

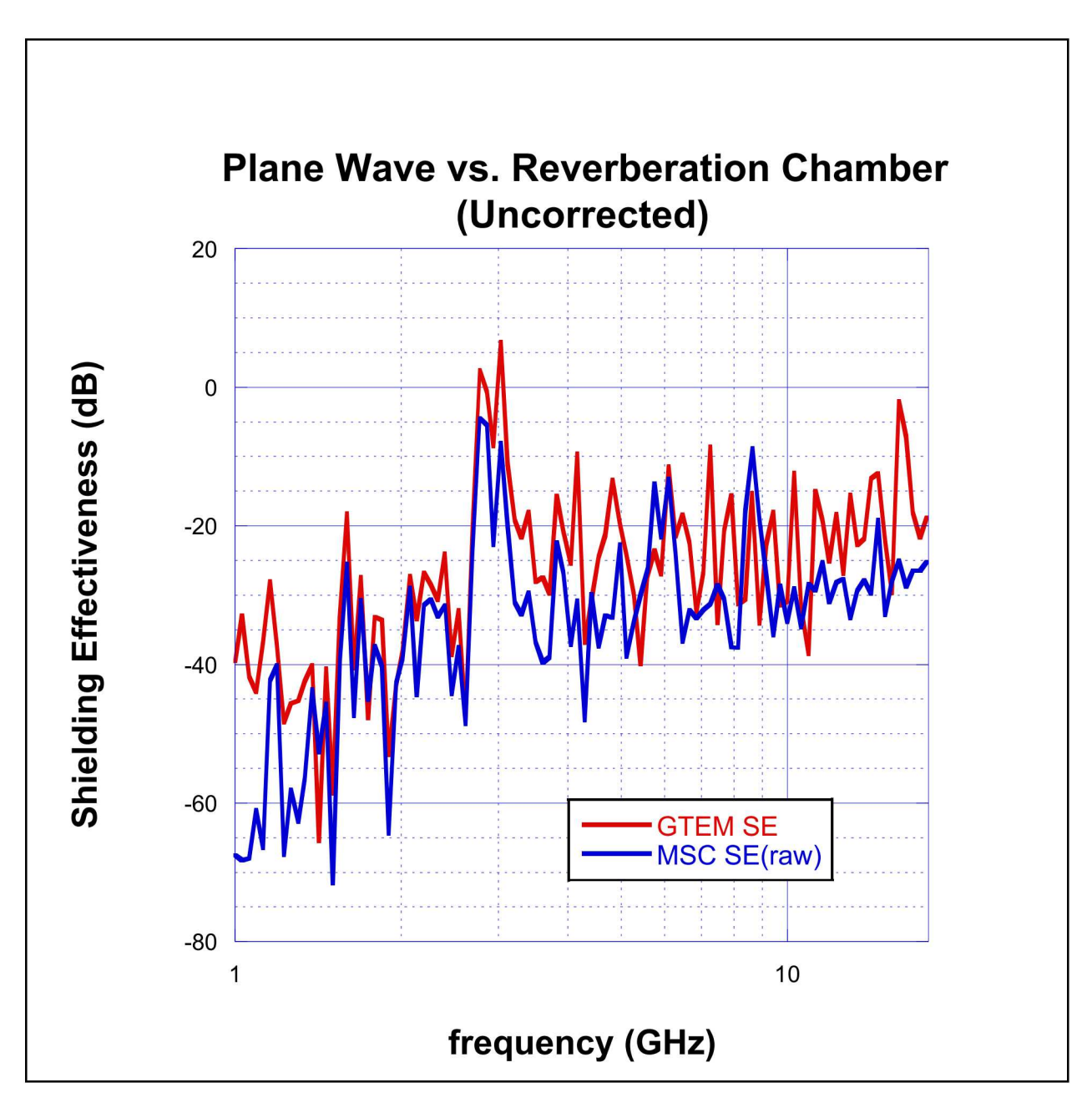


Figure 11: Uncorrected shielding effectiveness measurements. Below 1.5 GHz the GTEM SE is artificially degraded because the measurement instrumentation is at its noise floor.

Below about 1.5 GHz the two measurement data sets diverge significantly. This is the result of the fact that the received power of the internal monopole is below the noise floor of the measurement instrumentation. Shielding effectiveness is the ratio of received power inside the test object to the received power outside of it. When the true internal received power is at or below the noise floor of the measurement instrumentation, the numerator of this ratio becomes constant while the denominator continues to decrease. As a result, the ratio is artificially increased. The reverberation chamber data (aka MSC) do not show this effect because the external fields are significantly higher and the internal measurement is always above the

instrumentation noise floor. In future work a low noise amplifier will be added to the receiver side to mitigate this effect.

Above 1.5 GHz a consistent offset can be seen between the reverberation (MSC) chamber and GTEM results. The reverberation chamber makes the shielding effectiveness look overly optimistic relative to the actual threat environment. This is why a correction factor is needed when testing in a reverberation chamber.

As stated earlier, a correction factor has been published by researchers at NIST (Koepke, Hill, & Ladbury, 1996). Figure 12 shows a comparison of the GTEM and mode-stirred chamber SE results. The correlation between the two data sets is much improved with the correction factor applied.

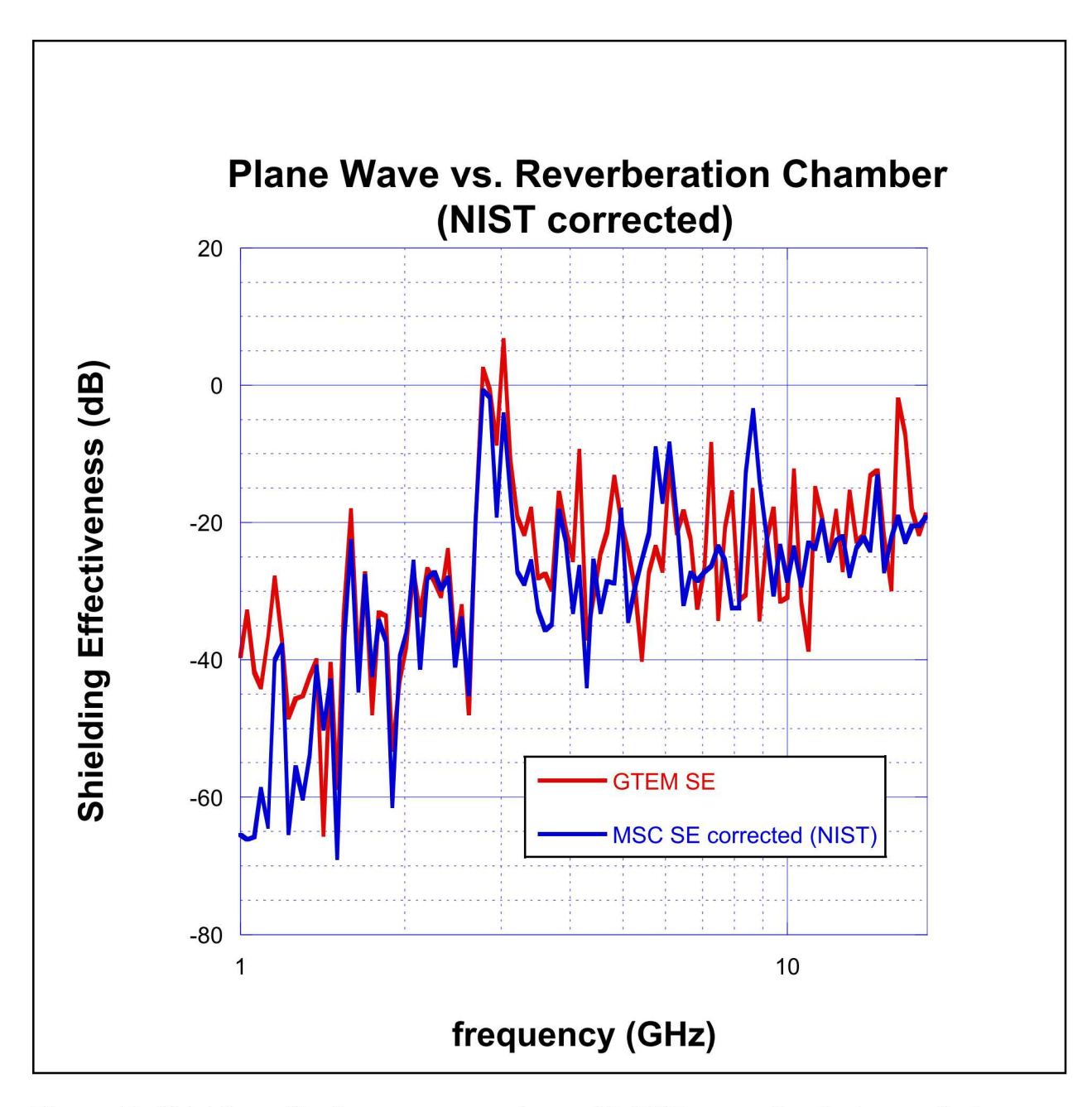


Figure 12: Shielding effectiveness comparison with NIST correction factor applied. Below 1.5 GHz the GTEM SE is artificially degraded because the measurement instrumentation is at its noise floor.

Sandia (Warne, et al) have also developed a correction factor based on an effective slot length. This method has been described in a previous report (Higgins, Hudson, Charley, Caldwell, & Sorensen, 2006). Figure 13 shows the same data as before, but with the Sandia $4L/\lambda$ factor applied.

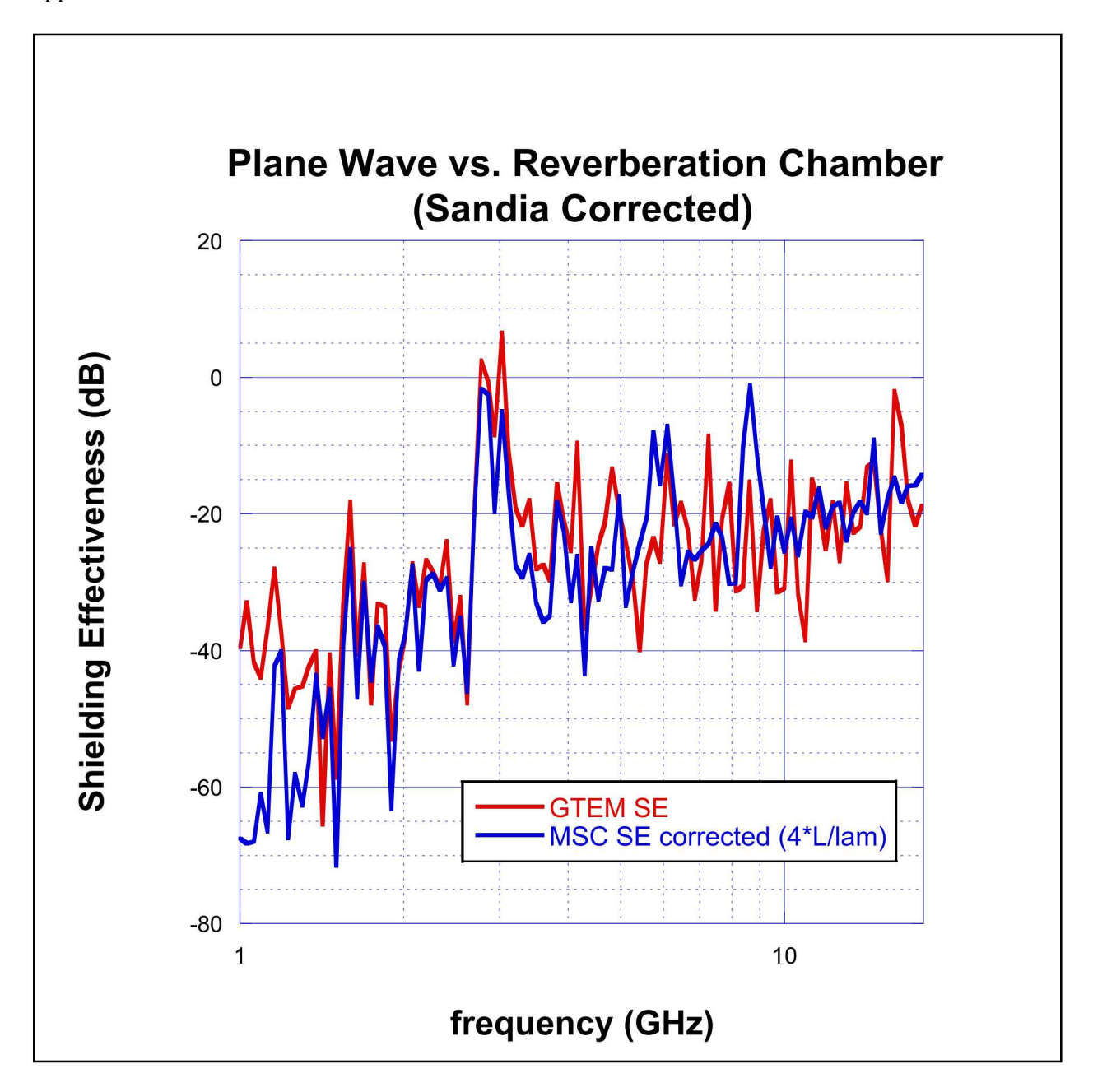


Figure 13: Shielding effectiveness comparison with Sandia correction factor applied. Below 1.5 GHz the GTEM SE is artificially degraded because the measurement instrumentation is at its noise floor.

The Warne slot gain factor results in a better correlation to the plane wave (GTEM) data, especially at high frequencies. These results support the use of the Sandia correction factor in NW testing.

2.2 Internal Stirrer Test

Many researchers advocate the use of a stirrer internal to the test object being tested. Sandia normally tests fully populated systems and use of an internal stirrer is not practical. Furthermore, the use of an internal stirrer tacitly assumes that the test frequencies are high enough that the interior of the test object is in reverberation. Nevertheless, it is of interest to compare shielding effectiveness results for the canonical test object used in this work. To this end, a small stirrer was constructed for the test object. This is shown in Figure 14.



Figure 14: Internal stirrer for the canonical test object

The internal stirrer pictured above was driven by a small battery powered electric motor. The shaft of the motor was constructed of a non-conductive material to avoid creating a conductive penetration. The stirrer rotation rate was about 3 times the rate of the main chamber stirrer. The dimensions of the test object are large enough that the cavity should be in reverberation over the entire frequency range tested.

The results of this investigation are shown in Figure 15. Three test cases were run. In the first case the internal stirrer was turning. In the second run the battery was disconnected and the stirrer stopped. The third case was with the stirrer removed entirely, although the non-

conductive shaft was left intact. Very little difference between the second and third cases can be seen. However, with the stirrer turning there is a substantial effect at low frequencies. Above the slot resonance frequency of 3 GHz, however, this effect is lost. Future work will focus on the effect of multiple internal sensors in computing the average internal field.

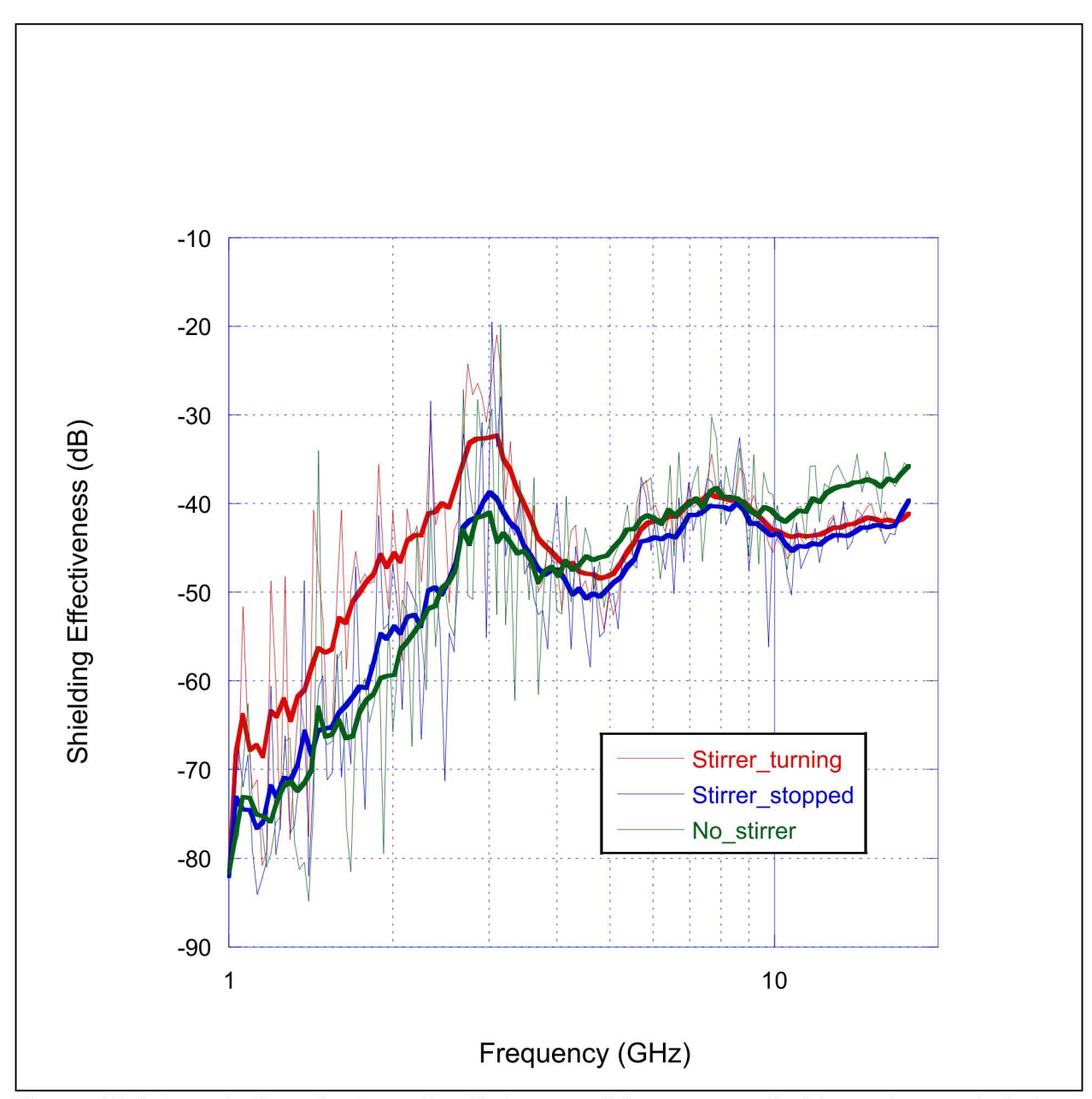


Figure 15: Internal stirrer test results. Data smoothing was applied to each case to help distinguish the data trends.

3. CONCLUSION

The results of calibration tests run on the Sandia reverberation chamber have been presented. The spatial variation of the electric field is shown to be less than 3 dB over the range of frequencies where the chamber is operated. The data show that the chamber can be operated as low as 100 MHz and still comply with the DO-160G and MIL-STD specifications. Against the more stringent IEC-61000-4-21 standard the lowest usable frequency would be 135 MHz. Sandia's chamber is usually operated only above 200 MHz.

Good correlation was found between the field estimation based on the wall sensors and measurements made with a calibrated field probe. The largest differences observed were of the order of 1.5 dB. However, these measurements were made with the field probe in a single location. Since the point to point variation within the working volume is of the order of 3 dB based on the calibration data, it is not clear that some of the difference observed is not simply due to the choice of field probe location. In future work the calibrated probe will be placed at multiple random locations within the working volume.

The Sandia $(4L/\lambda)$ factor was found to provide the best correction for relating the reverberation and plane wave environments. The NIST model also gave excellent results. Future work should continue the measurements with multiple slots and additional types of apertures. Future work should also include multiple angles of incidence for the plane wave, as was done in the initial Higgins work.

Finally, the effect of an internal stirrer on reverberation chamber measured shielding effectiveness has been investigated. It was found that presence of the stirrer can significantly affect the shielding effectiveness measurement at low frequency. At high frequencies the results are more or less equivalent.

4. REFERENCES

- DO-160G. (2010). Environmental Conditions and Test Procedures for Airborne Equipment. Washington, DC: RTCA, Inc.
- Higgins, M. B., & Charley, D. R. (2007). Electromagnetic Radiation (EMR) Coupling into Complex Systems Aperture Coupling into Canonical Cavities in Reverberant and Anechoic Environments and Model Validation (SAND2007-7391). Sandia National Laboratories.
- Higgins, M. B., Hudson, H. G., Charley, D. R., Caldwell, M., & Sorensen, E. S. (2006). *EM-1: ALCM Electromagnetic Transfer Function Test (SAND2006-3472).* (report is OUO).
- Hill, D. A. (2009). Electromagnetic Fields in Cavities. Hoboken: John Wiley and Sons.
- IEC 61000-4-21. (2011). Electromagnetic compatibility(EMC) Part 4-21: Testing and Measurement Techniques Reverberation Chamber Test Methods. Geneva, Switzerland: IEC.
- Koepke, G. H., Hill, D. A., & Ladbury, J. (1996). Directivity of the Test Device in EMC Measurements. *IEEE Transactions on Electromagnetic Compatibility*, 165-172.
- MIL-STD-461F. (2007). Requirements for the Control of Electromagnetic Interference Characteristics of Subsystems and Equipment. US Department of Defense.

5. DISTRIBUTION

Lawrence Livermore National Laboratory Attn: N. Dunipace (1) P.O. Box 808, MS L-795 Livermore, CA 94551-0808

1	MS0557	David Epp Steven Glover Mark Jursich Michael Dinallo Matthew Halligan Lorena Basilio	1522
1	MS1152		1353
1	MS1152		1353
1	MS1152		1354
1	MS1152		1353
1	MS1152 MS0899	Lorena Basilio Technical Library	1352 9536 (electronic copy)

